Hindawi
Mathematical Problems in Engineering
Volume 2022, Article ID 1112646, 11 pages
https://doi.org/10.1155/2022/1112646

Research Article

Signal-in-Space and Positioning Performance of BDS Open Augmentation Service

Liang Chen,[1] **Guangyu Zhou**,[1] **Guo Chen**,[2] **Weibin Sun**,[2] **and Luotian Pan**[3,4]

[1]*School of Electronic and Information Engineering, Beihang University, Beijing 100191, China*
[2]*GNSS Research Center, Wuhan University, Wuhan 430079, China*
[3]*School of Land Science and Technology, China University of Geosciences Beijing, Beijing 100083, China*
[4]*Beijing Key Laboratory of Urban Spatial Information Engineering, Beijing 100038, China*

Correspondence should be addressed to Guo Chen; guo_chen@whu.edu.cn

Received 11 February 2022; Accepted 10 March 2022; Published 1 April 2022

Academic Editor: Xinyuan Jiang

As a typical augmentation satellite system for centimeter-level positioning, PPP (Precise Point Positioning) service based on PPP-B2b signal of China's new generation BeiDou system (BDS-3) was released for Asia-Pacific area on July, 2020. This paper first introduces the recovery theory of PPP-B2b SSR (State Space Representation) messages and then implements a real-time PPP-B2b precise positioning terminal to decode and obtain the PPP-B2b SSR orbit, clock, and biases. On those bases, the coverage, signal-in-space, and positioning performance of PPP-B2b SSR are evaluated. The results show that PPP-B2b SSR of BDS-3 can cover the most area of 50°E-180°E, 30°S-70°N and improve signal-in-space accuracy significantly. The improvement rate on BDS clock offset can reach 77%, which far exceeds average 40% improvement on BDS orbit, while it is opposite for GPS with 80% improvement rate on orbit and 61% on clock offset. Average SISRE (signal-in-space range error) of PPP-B2b SSR is better than 10 cm. The 95% positioning results show that centimeter- to decimeter-level positioning can be achieved after a few minutes of convergence based on PPP-B2b SSR, which satisfies the BDS open service performance standard. Comparing to BDS PPP based on PPP-B2b SSR, BDS + GPS PPP can promote convergence significantly with average 40% improvement rate for 95% epochs and can further improve positioning accuracy with 30%-35% improvement rate in horizontal and 10%–15% in vertical direction.

1. Introduction

Currently, there are two technology paths of GNSS precise positioning, i.e., GNSS OSR (Observation Space Representation) and SSR (State Space Representation) [1]. RTK (Real-Time Kinematic) is one typical OSR technology and another is PPP (Precise Point Positioning) for SSR [2]. As is known to all, PPP can obtain the absolute positions and time information for global area without relying on nearby reference stations, which is the main advantage comparing to RTK [3]. PPP realizes a user precise positioning based on precise GNSS orbit and clock messages and carrier phase observations, where the ionospheric-free (IF) combinations are usually used to eliminate ionospheric delay in signal transmission [4]. It needs about 15–30 minutes to convergence undifferenced (UD) ambiguity of PPP before obtaining a centimeter-level accuracy [5], while RTK can achieve instantaneous precise positioning. With the construction and upgrading of GNSS system, more and more GNSS provide the open precise positioning services, like the Galileo HAS (High Accuracy Service), QZSS (Quasi-Zenith Satellite System), CLAS (Centimeter Level Augmentation Service), and BDS PPP service [6]. The realization path of those open services is basically the same, i.e., receiver side can reconstruct precise augmentation messages by correcting those open SSR messages including orbit, clock, and atmospheric corrections to broadcast ephemeris.

Galileo HAS, broadcasting high-accuracy SSR corrections by E6-B signal for Galileo and GPS signals, will provide initial service in 2021 and full service in 2024 [7]. The services include standard global PPP service and regional rapid positioning service by additional regional atmospheric,

biases corrections, etc. [7]. QZSS CLAS, based on SSR, is an open nation-wide PPP-RTK service for Japan and has been operational since November 2018 [8], which can augment QZSS, GPS, and Galileo signals currently and will provide augmentation service for GLONASS in the future [9]. The satellite system developed by Australia and New Zealand jointly will also open the real-time PPP service through one Inmarsat satellite in 2023 [10]. GLONASS plans to have a commercial PPP service using its L3 signal in 2030 [11].

BDS-3, China's new generation satellite navigation system, was opened on July 31st, 2020, and can provide various global and regional services [12, 13]. BDS-3 constellation includes 3 GEO (Geostationary Earth Orbit), 3 IGSO (Inclined Geosynchronous Orbit), and 24 MEO (Medium Earth Orbit) satellites. BDS-3 is downward compatible with BDS-2 B1I/B3I signals, while broadcasting those new signals of B1C/B2a/B2b [13]. Currently, BDS PPP service based on PPP-B2b signal can achieve decimeter-level dynamic positioning and centimeter-level static positioning for Asia-Pacific area [14]. ISO 18197 is an international standard specification in space systems category [15] and describes those requirements for space-based centimeter-level positioning services [16]. According to this specification, an augmentation satellite system for centimeter-level positioning consists of GNSS, augmentation satellites, augmentation satellite control stations, ground reference points, positioning augmentation centers, and user terminals as shown in Figure 1. So BDS PPP service based on BDS-3 PPP-B2b signal is a typical augmentation satellite system for centimeter-level positioning.

BDS PPP-B2b SSR messages include satellite orbit, satellite clock corrections, and DCB (differential code bias) [14], which are modulated in the PPP-B2b signal and broadcasted to receiver by 3 GEOs of BDS-3 constellation. According to the design, the structure of BDS-3 PPP-B2b signal can encode those SSR corrections of BDS, GPS, GLONASS, and Galileo [14]; however, only SSR corrections of BDS-3 and GPS are broadcasted for users in and around China currently [17]. BDS PPP-B2b SSR messages can correct the CNAV1 NAV ephemeris of BDS B1C signal and the LNAV NAV ephemeris of GPS L1C/A signal [13]. Receiver can recover those SSR corrections to real-time PPP-B2b ephemeris by matching the broadcast ephemeris and achieve precise positioning combined with carrier phase and pseudorange observations.

The structure of this paper is as follows: firstly, the methodology part introduces the recovery theory of PPP-B2b SSR messages and realizes a real-time PPP-B2b precise positioning terminal to decode and obtain the PPP-B2b SSR orbit, clock, biases, etc. On those bases, the coverage of BDS PPP and BDS + GPS combined with PPP based on PPP-B2b SSR is evaluated. The orbit, clock, and SISRE are also analysed. Part of GNSS tracking stations in coverage area are used to analyse the real-time positioning performance of PPP-B2b messages by postprocessing kinematic mode, including convergence and accuracy. Experiment results and conclusions are provided in Conclusions.

2. Methodology

PPP is a method based on observations of a single receiver and externally known precise augmentation messages (satellite orbit, clock offset, atmospheric delay, and biases) to resolve receiver-side unknown parameters including precise coordinates, receiver clock offset, atmosphere, and ambiguity [5]. The observation and method of PPP-B2b SSR messages recovery are introduced in this section; then a real-time PPP-B2b precise positioning terminal is realized to encode and obtain the PPP-B2b SSR orbit, clock, biases, etc.

2.1. Observations. GNSS raw pseudorange and carrier phase observations of different frequencies are as follows [18]:

$$\begin{aligned} p_{r,j}^{s} &= \rho_r^s + c \cdot \left(\mathrm{d}t_r + d_{r,j}\right) - c \cdot \left(\mathrm{d}t^s + d_j^s\right) + I_{r,j}^s + T_r^s + \varepsilon_{r,p,j}^s, \\ \varphi_{r,j}^{s} &= \rho_r^s + c \cdot \left(\mathrm{d}t_r + \delta_{r,j}\right) - c \cdot \left(\mathrm{d}t^s + \delta_j^s\right) - I_{r,j}^s + T_r^s + \lambda_j \cdot N_{r,j}^s + \varepsilon_{r,\varphi,j}^s, \end{aligned} \tag{1}$$

where superscripts s and r identify one satellite and one receiver, respectively. p and φ represent the pseudorange and carrier phase observations. j is the frequency and the corresponding wavelength λ_j. Further, ρ is the signal travelled geometric distance from satellite broadcasting to receiver reception, and $\mathrm{d}t_r$ and $\mathrm{d}t^s$ are clock offsets in receiver- and satellite-side. c is the velocity of light in vacuum; I_r^s is ionosphere delay; T is troposphere. N is ambiguity. ε is observation noise and multipath. $d_{r,j}$ and d_j^s are receiver-dependent and satellite-dependent instrumental delay biases in pseudorange; $\delta_{r,j}$ and δ_j^s are receiver-dependent and satellite-dependent instrumental delay biases in carrier-phase observations, respectively.

There is no atmosphere augmentation message in BDS-3 PPP-B2b SSR currently, so the ionospheric delay can be eliminated by double-frequency IF combination [4] and tropospheric delay can be estimated as a zenith wet delay parameter using a wet mapping function as shown in equation (1).

2.2. SSR Messages Recovery. The PPP-B2b SSR message types are shown in Table 1.

A group of IOD (issue of data) parameters are designed to build the interrelationship among those different message types, including IOD SSR (IOD of SSR), IODP (IOD of

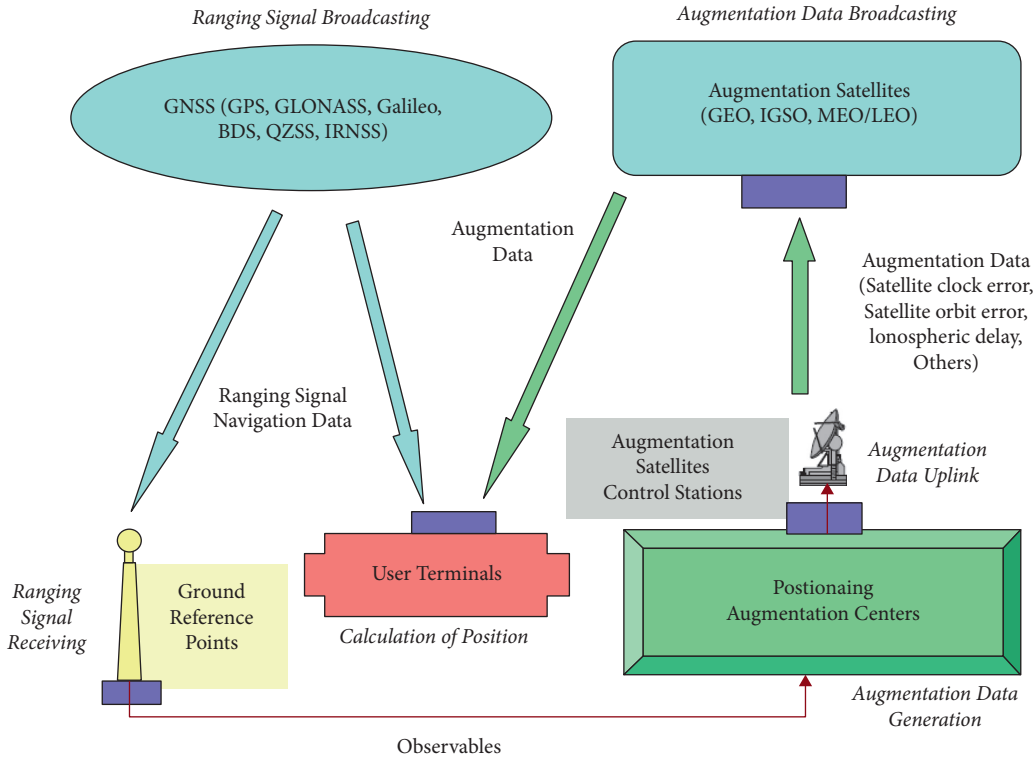

Figure 1: ISO 18197 typical augmentation satellite system for centimeter-level positioning [16].

Table 1: SSR message types in PPP-B2b [14].

Message type (in decimal)	Correction content
1	Satellite mask
2	Satellite orbit correction and user range accuracy
3	Differential code bias
4	Satellite clock correction
5	User range accuracy index
6	Clock correction and orbit correction–combination 1
7	Clock correction and orbit correction–combination 2
8–62	Reserved
63	Null

satellite pseudorandom noise mask), IODN (IOD of navigation data), and IOD Corr (IOD of orbit and clock correction). Currently, only SSR corrections of BDS-3 and GPS satellites are broadcasted to correct the CNAV1 NAV message of the BDS B1C signal and the LNAV NAV message of the GPS L1C/A signal [14].

The parameter of IODN is used to search the corresponding navigation ephemeris by matching with the IODC (IOD of clock) parameter in BDS CNAV1 message of B1C signal and IODC in GPS LNAV message, respectively. The process can be described as follows: firstly comparing the parameters of PPP-B2b IODN and navigation messages IODC, a failure matching means that the navigation messages have been updated, so the previous navigation message should continue to be used until the PPP-B2b IODN is updated and matches the IODC. After matching the PPP-B2b SSR correction messages and navigation messages successfully, the next step is to recover the absolute SSR messages of satellite precise orbit, clock, and differential code bias.

2.2.1. Orbit Recovery. According to ICD (Interface Control Document) of BDS PPP-B2b, the orbit corrections of radial-, along-, and cross-direction in satellite orbit coordinate system are provided, which can be noted as $\delta\mathbf{O}$. Those orbit parameters in broadcast ephemeris express the position of the satellite in Earth coordinate system, the orbit correction vector $\delta\mathbf{O}$ should be translated to Earth coordinate system by the following equation:

$$\begin{aligned}
\mathbf{e}_{\text{radial}} &= -\frac{\mathbf{X}}{|\mathbf{X}|},\\
\mathbf{e}_{\text{cross}} &= -\frac{\mathbf{X}\times\mathbf{V}}{|\mathbf{X}\times\mathbf{V}|},\\
\mathbf{e}_{\text{along}} &= -\mathbf{e}_{\text{cross}}\times\mathbf{e}_{\text{radial}},\\
\delta\mathbf{X} &= \left[\begin{array}{ccc}\mathbf{e}_{\text{radial}} & \mathbf{e}_{\text{along}} & \mathbf{e}_{\text{cross}}\end{array}\right]\cdot\delta\mathbf{O},
\end{aligned} \tag{2}$$

where $\mathbf{X}$ and $\mathbf{V}$ are the satellite position and velocity vector calculated by broadcast ephemeris, respectively; ($\mathbf{e}_{\text{radial}}$, $\mathbf{e}_{\text{along}}$, $\mathbf{e}_{\text{cross}}$) is the projection vector between those two coordinate systems; $\delta\mathbf{X}$ is satellite orbit corrections in earth coordinate system.

Then the corrected orbit $\mathbf{X}_{\text{prec}}$ can be obtained by

$$\mathbf{X}_{\text{prec}} = \mathbf{X}_{\text{brdc}} + \boldsymbol{\delta}\mathbf{X}. \tag{3}$$

2.2.2. Clock Recovery. Like orbit corrections, clock corrections in PPP-B2b SSR are relative to clock offset calculated by broadcast ephemeris. The corrected satellite clock can be obtained by

$$\mathrm{d}t_{\text{prec}} = \mathrm{d}t_{brdc} - \frac{C_0}{c}, \tag{4}$$

where $\mathrm{d}t_{\text{prec}}$ is the corrected precise clock of PPP-B2b SSR and $\mathrm{d}t_{brdc}$ is the clock parameter from broadcast ephemeris, respectively. c is the velocity of light; C_0 is the clock corrections of PPP-B2b SSR.

2.2.3. DCB. The differences among signal tracking modes lead to offsets in different frequency observations. PPP-B2b corrections also provide the DCB correction parameters to eliminate the differential code bias as

$$\widetilde{l} = l - DCB, \tag{5}$$

where l is the original pseudorange observations and $\widetilde{l}$ is the corrected observations. When using double-frequency signals for PPP, the IF combination DCB corrections in (6) can be used to correct the satellite clock of PPP-B2b SSR directly.

$$\widetilde{dt}_{\text{prec}} = \mathrm{d}t_{\text{prec}} - \frac{\gamma \cdot DCB_1 - DCB_2}{\gamma - 1}, \tag{6}$$

where $\widetilde{dt}_{\text{prec}}$ is the PPP-B2b real-time satellite clock bias corrected by DCB, $\gamma = f_1^2/f_2^2$; DCB_1 and DCB_2 are the DCB of those two frequencies.

2.3. PPP-B2b Decoding. Based on BDS PPP-B2b signal and methodology above, PPP-B2b decoding process at the terminal is shown in Figure 2. The terminal is mainly composed of a RF (radio frequency) front-end and signal processing and information processing modules. The module of RF front-end receives the signal from antenna and obtains an intermediate frequency digital signal after downconversion, filtering, and sampling. The signal processing module demodulates the digital signal to obtain GNSS observations, broadcast ephemeris, and PPP-B2b SSR messages. The information processing module mainly recovers the orbit, clock, and bias based on PPP-B2b SSR and broadcast ephemeris and then calculates the positioning information including coordinates, clock, and troposphere.

3. Evaluation of BDS PPP-B2b SSR

For an open service provided by GNSS, the coverage and signal-in-space performance are key service indicators. According to basic methodology of PPP and signal beam range, the coverage of PPP-B2b SSR is shown in this part. Then the orbit and clock accuracy are evaluated independently. The SISRE (signal-in-space range error), the combination of orbit and clock error, is also analysed.

3.1. Coverage. From Table 1, the BDS-3 can provide the PPP service for Asia-Pacific users via PPP-B2b signal broadcasted by three GEO satellites. There are many conditions constraining PPP-B2b service coverage like the coverage of BDS-3 three GEOs, the number, availability, and space geometry of visible satellites matched with SSR messages successfully. From (1), the estimated parameters include three positions, one receiver clock offset, one troposphere residual, and ambiguities in single-GNSS PPP, while an ISB (intersystem bias) parameter should be added into BDS + GPS PPP in order to realize time synchronization [5]. So minimum satellite number for single-GNSS and BDS + GPS PPP is five and six, respectively. In addition, the requirements for correction targets: the BDS radio navigation satellite service (RNSS) performance meets the "BDS open service performance standard (Version 3.0)" [13]; GPS service performance meets the requirements of "GPS Standard Positioning Service Performance Standard (Version 5.0)" [19]. Therefore, the PDOP 6 is also selected as a condition for coverage analysis.

The broadcast ephemeris and PPP-B2b SSR correction messages of a regression period of BDS (7 days) are used to evaluate the coverage of BDS PPP service. The global area is divided into regular grids (such as $1^\circ \times 1^\circ$). With 300s sampling interval and 7° mask elevation angle, PDOP of each grid point in the regression period is calculated based on available satellites corrected by PPP-B2b SSR messages. Then availability percentage of PDOP less than certain conditions in each grid point is statistically analysed to evaluate the coverage of BDS PPP-B2b SSR.

Figures 3 and 4 give the service coverage of BDS and BDS + GPS PPP based on PPP-B2b SSR messages under the condition of PDOP ≤6 from DOY (day of year) 346 to 353, 2020, respectively. From Figure 3, we can find that the availability all over China can reach more than 90% under the condition of PDOP ≤6 and the service coverage is about 65°E–160°E, 15°S–70°N. After combining GPS, the coverage is further expanded to 50°E–180°E, 30°S–70°N.

3.2. Orbit and Clock. The basic principle of BDS-3 PPP-B2b augmentation service is to provide more precise ephemeris (orbit, clock, and biases) than broadcast ephemeris to improve SISRE accuracy. So the accuracy of satellite orbit and clock offset is the key technical indicators of PPP-B2b SSR ephemeris products, which determine the PPP positioning performance including accuracy and convergence.

We need to note that the satellite orbits corrected by PPP-B2b SSR message refer to satellite's APC (antenna phase center) [17], while the precise orbit products provided by IGS refer to satellite's CoM (center-of-mass) [20]. Therefore, the satellite APC positions need to be converted to the satellite CoM positions by applying PCO (phase center offset) corrections [21], where GPS satellite's PCO is provided by IGS14.atx [22] and BDS-3 satellite's PCO is provided by BeiDou official website (https://en.beidou.gov.cn/SYSTEMS/Officialdocument/201912/P020200323536112807882.atx). The accuracy of BDS PPP-B2b clock is analysed by quadratic-difference method

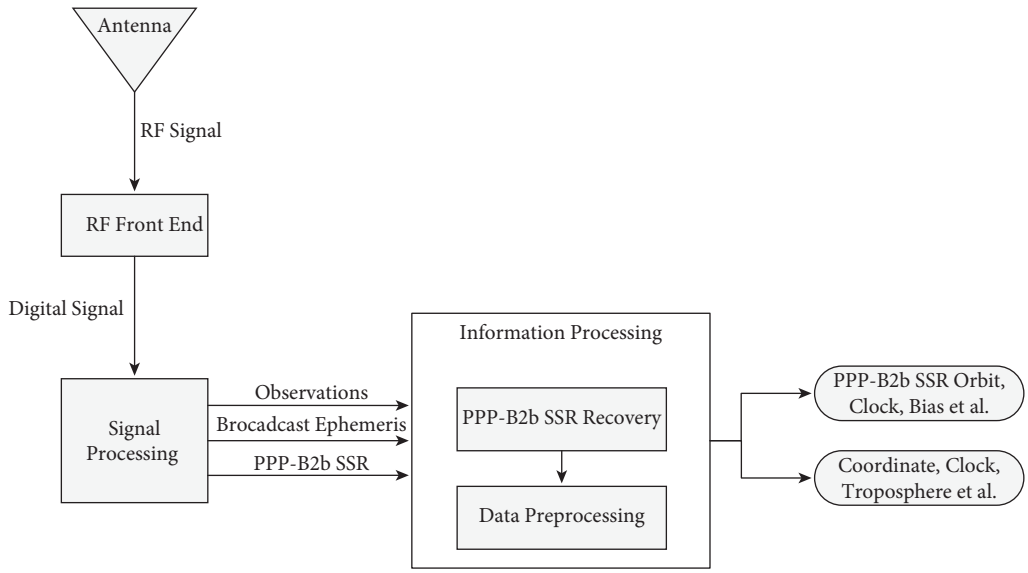

Figure 2: Frame of BDS PPP-B2b decoding process at the terminal.

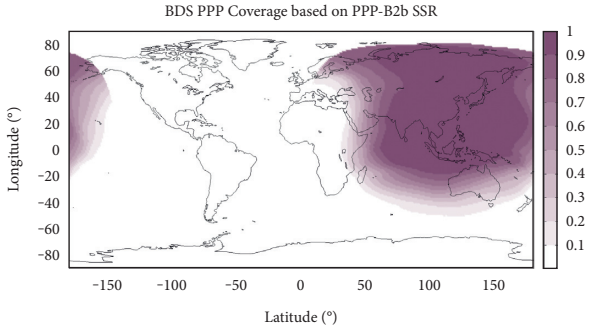

Figure 3: The service availability of BDS PPP based on PPP-B2b SSR (PDOP ≤6).

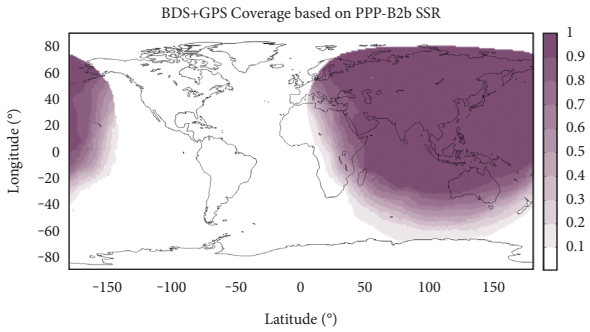

Figure 4: The service availability of BDS + GPS PPP based on PPP-B2b SSR (PDOP ≤6).

[4, 23, 24]. As shown in (7), one satellite is chosen as the reference to remove the datum bias of different products. After deducting datum time bias, the quadratic difference can be obtained by making difference further between PPP-B2b clock and precise clock products.

$$\Delta\nabla \mathrm{d}t^{S}_{B2b-GBM} = \left(\mathrm{d}t^{S}_{B2b} - \mathrm{d}t^{S\_\mathrm{ref}}_{B2b}\right) - \left(\mathrm{d}t^{S}_{GBM} - \mathrm{d}t^{S\_\mathrm{ref}}_{GBM}\right). \quad (7)$$

Then STD can be obtained by

$$STD = \sqrt{\frac{\sum_{i=1}^{n}\left(\Delta\nabla \mathrm{d}t^{S}_{i} - AVE\left(\Delta\nabla \mathrm{d}t^{S}\right)\right)^{2}}{n-1}}, \quad (8)$$

where $\Delta\nabla \mathrm{d}t^{S}_{i}$ is the quadratic difference in i-th epoch. $AVE(\Delta\nabla \mathrm{d}t^{S})$, the average of these quadratic clock differences, includes not only initial clock offset biases caused by pseudorange but also DCB caused by different signals, which can be absorbed by float ambiguity parameter. Therefore, STD of clock quadratic difference is usually used to evaluate its accuracy. GNSS precise data processing based on IF dual-frequency combination observations leads to DCB of IF combinations existing in most of IGS clock products [25]. As we all know, the DCB can keep stable for a long time [26–28]. From (7) and (8), it is can be found that the DCB will be absorbed by $AVE(\Delta\nabla \mathrm{d}t^{S})$, and whether the dt^{S}_{B2b} is calculated from original equation (4) or DCB corrected equation (6) will not affect final clock accuracy analysis.

In order to verify the accuracy of BDS PPP-B2b SSR messages, GBM GNSS precise orbit and clock provided by GFZ (German Research Center for Geosciences) are chosen as reference. Compared to other IGS Analysis Centers products, GBM products accuracy is about 1–3 cm for GPS and 4–7 cm for BDS non-GEO, and BDS orbit accuracy with SLR calibrating is less than 10 cm [25]. The PPP-B2b SSR messages of day of year (DOY) 346 to 353 of 2020 are analysed and the broadcast ephemeris accuracy in same time period is also evaluated as comparison.

Figures 5 and 6 show BDS and GPS orbit errors corrected by BDS PPP-B2b SSR in satellite orbit coordinate system, respectively. Table 2 shows the statistic results of BDS-3 and GPS broadcast ephemeris and PPP-B2b SSR message comparing to GBM precise products. It can be obtained from Figures 5 and 6 that GPS orbit of PPP-B2b SSR is better than BDS, especially in radial-direction. According to the statistic in Table 2, BDS broadcast orbit accuracy is about

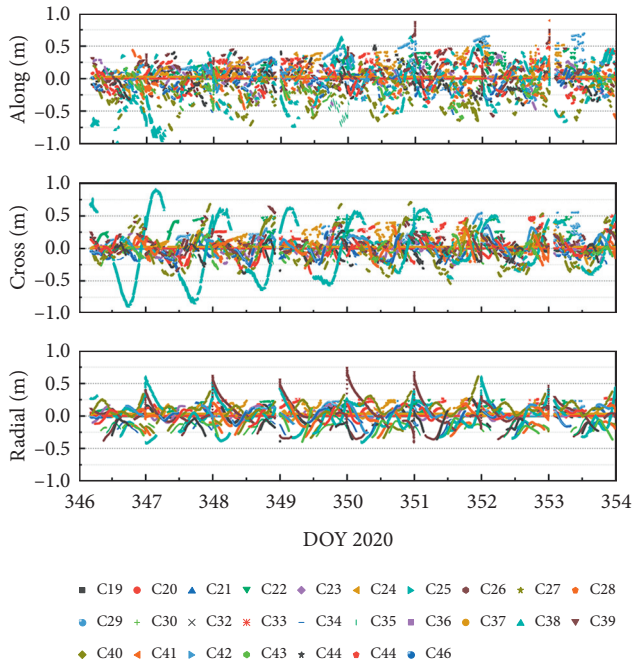

Figure 5: BDS orbit errors corrected by BDS PPP-B2b in along-direction, cross-direction, and radial-direction.

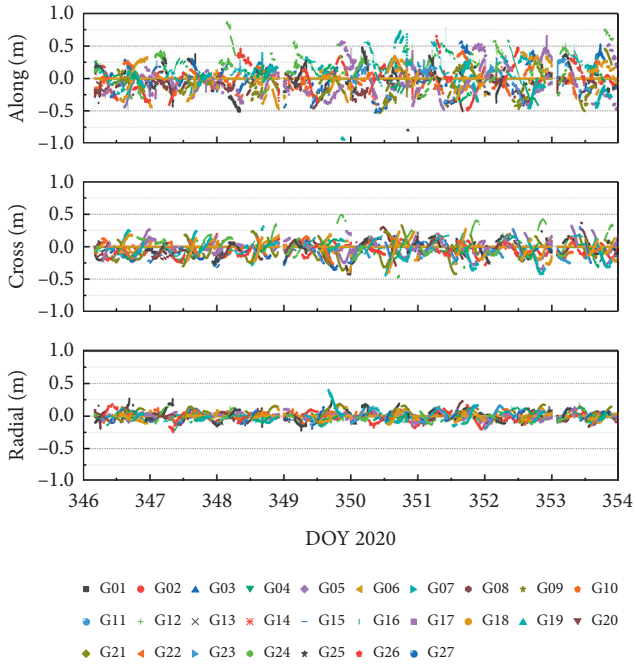

Figure 6: GPS orbit errors corrected by BDS PPP-B2b in along-direction, cross-direction, and radial-direction.

30–35 cm in along- and cross-direction and 15 cm in along-direction and clock offset is about 0.9 ns. After PPP-B2b SSR correction, the BDS orbit accuracy can be improved to 22.60 cm, 16.31 cm, and 8.31 cm in along-, cross-, and radial-direction, and clock offset accuracy can achieve 0.21 ns. For GPS, the orbit accuracy is about 19.34 cm, 11.79 cm, and 6.10 cm in along-, cross-, and radial-direction, and clock offset accuracy is about 0.30 ns. It is obvious that the improvement rate of PPP-B2b SSR on BDS clock offset can reach 77%, which far exceeds about 40% improvement on BDS orbit. While it is opposite for GPS, the improvement rate on orbit can reach about 80% exceeding 61% on clock offset. We can also find from Table 2, due to the use of intersatellite links, the accuracy of BDS-3 broadcast ephemeris is better than GPS.

3.3. Signal-in-Space Accuracy. From (1), we can find that users pay more attention on projection error in the line-of-sight direction from the satellite to receiver, which effects residuals in normal equation. Signal-in-Space Range Error (SISRE) is a statistical parameter of precise ephemeris projection errors [4], and calculation formula is as follows [29]:

$$SISRE = \sqrt{(\alpha \cdot \mathrm{d}R - c \cdot \mathrm{d}t)^2 + \frac{\left(\mathrm{d}A^2 + \mathrm{d}C^2\right)}{\beta}}, \quad (9)$$

where dR, dA, dC are radial-, along-, and cross-direction orbit error in satellite orbit coordinate system, respectively; dt is the clock bias; c is the velocity of light in vacuum. According to methodology of SISRE, the different satellite orbit altitudes determinate the coefficient α and β, which are shown in Table 3. Equation (9) and the coefficients of Table 3 show the radial-direction orbit error and clock bias are main factors affecting SISRE. dR and dt influence each other and keep self-consistent for unified track and clock difference products.

Figures 7 and 8 show SISRE time series and average of PPP-B2b SSR message from DOY 346 to 353, 2020. From Figure 7, most of BDS and GPS SISRE are less than 20 cm and can keep stable over time. According to statistic in Figure 8, the average SISRE of BDS-3 and GPS is 7.10 cm and 7.58 cm, respectively.

4. Performance of PPP-B2b Precise Positioning

The coverage and signal-in-space performance of BDS PPP-B2b SSR have been analysed above. Part of GNSS tracking stations in coverage area are used to assess the real-time kinematic positioning performance of PPP-B2b messages by postprocessing analysis, including convergence and accuracy.

4.1. Data and Strategy. The mission of iGMAS (international GNSS monitoring and assessment system) is to build global tracking stations to monitor and evaluate GNSS service performance [30]. Part stations of iGMAS in the coverage of BDS PPP-B2b signal are selected to evaluate the BDS-3 PPP service performance, which are shown in Figure 9 and can track all the open service signals of GNSS. Those data of DOY 340–353, 2020 are analysed following the processing strategy shown in Table 4. As mentioned above, the precise orbits recovered by PPP-B2b messages refer to the APC, so

Table 2: Accuracy statistics of BDS-3 and GPS broadcast ephemeris and PPP-B2b SSR message.

Type		Orbit RMS (cm)			Clock bias STD (ns)
		Along	Cross	Radial	
BDS-3	BRDC	33.30	31.55	15.43	0.90
	PPP-B2b SSR	22.60	16.31	8.31	0.21
Improvement rate		32%	48%	46%	77%
GPS	BRDC	110.02	44.23	38.31	0.77
	PPP-B2b SSR	19.34	11.79	6.10	0.30
Improvement rate		82%	73%	84%	61%

Table 3: SISRE coefficients of BDS and GPS.

Satellite		Orbit Altitude (km)	α	β
BDS	GEO/IGSO	35786	0.99	127
	MEO	21528	0.98	54
GPS		20200	0.98	49

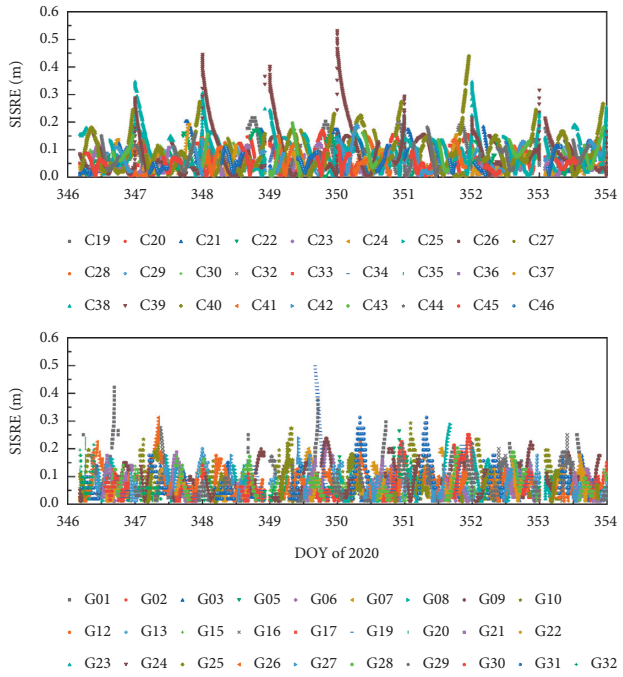

Figure 7: BDS and GPS SISRE time series of BDS PPP-B2b SSR message.

there is no need to correct the satellite-dependent PCO in precise positioning process based on PPP-B2b SSR.

4.2. Positioning Performance. Bases on those station's positioning results in different days, previous-4-hours including convergence period are analysed based on the following rules:

(1) The previous-4-hours start from the first epoch which can achieve positioning based on PPP-B2b SSR

(2) All those positioning results in the previous-4-hours regardless the different stations and epoch time formed a data pool

(3) The positioning errors of the data pool at same epoch in the previous-4-hours are sorted from small to large

(4) Then count the positioning error of mean, 68% and 95% epoch to analyse the positioning convergence and accuracy

Figures 10 and 11 show the previous-4-hours BDS and BDS + GPS PPP convergence statistic results based on BDS PPP-B2b SSR, where the red, blue, and black lines are the mean, 68%, and 95% statistical results, respectively. The convergence condition, coming from newest BDS open service performance standard [13], is shown as red dotted line, which is 30 cm in horizontal and 60 cm in vertical direction for BDS PPP and 20 cm and 40 cm for BDS + GPS

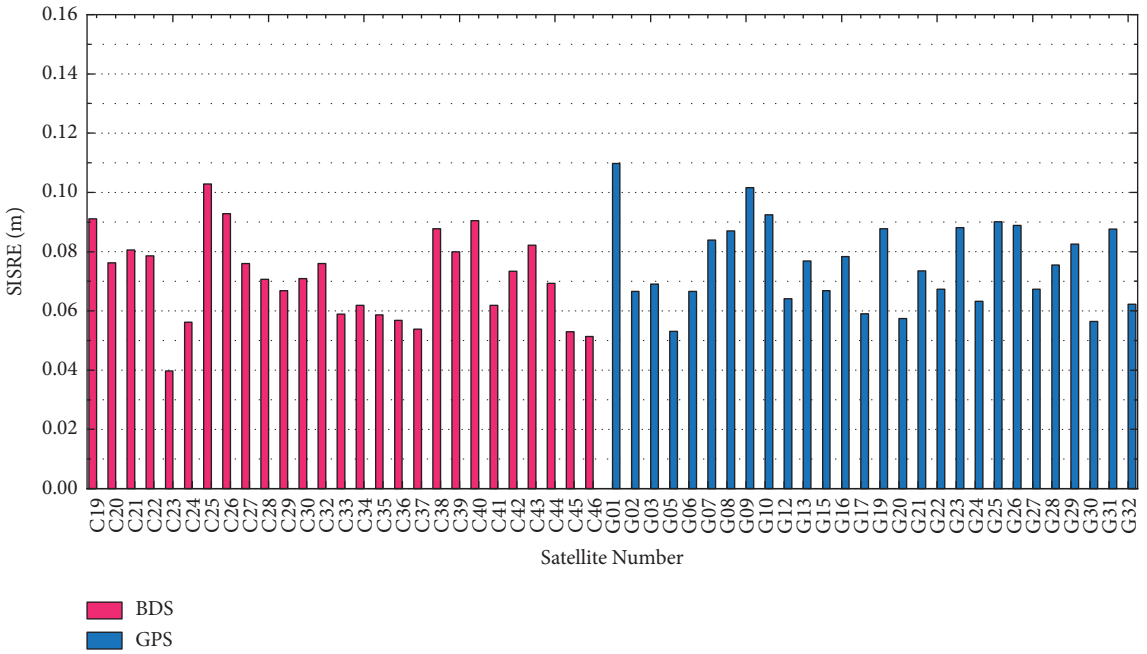

Figure 8: Average of BDS-3 and GPS SISRE of PPP-B2b SSR message.

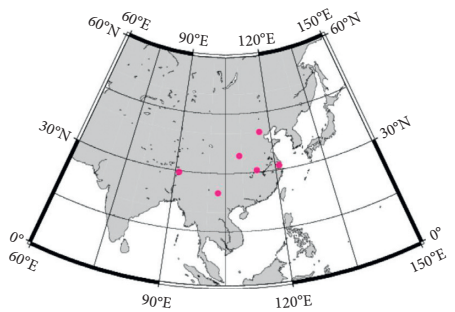

Figure 9: Distribution of tracking station.

Table 4: Estimation strategy of precise positioning receiver based on BDS PPP-B2b.

Parameters	Model
Observations	UD IF carrier-phase + pseudorange BDS-3: B1I + B3I GPS: L1 + L2 Interval: 30 s Elevation mask: 10°
Prior information	Pseudorange 1.0 m; carrier-phase 0.02 cycles
Observation weight	$p = 1$, elevation >30° $p = 2\sin$ (elevation), elevation ≤30° [31]
Ocean tides Earth solid tides	IERS conventions 2003
Phase wind-up	Correction [32]
Relativistic effects	Correction
Adjustment method	Square-root information filter [4]
Receiver clock offset	Estimated as white noise
Ambiguity	Float
Troposphere delay	Saastamoinen + GMF Single epoch random-walk process
ISB	Estimated as random-walk process [5]

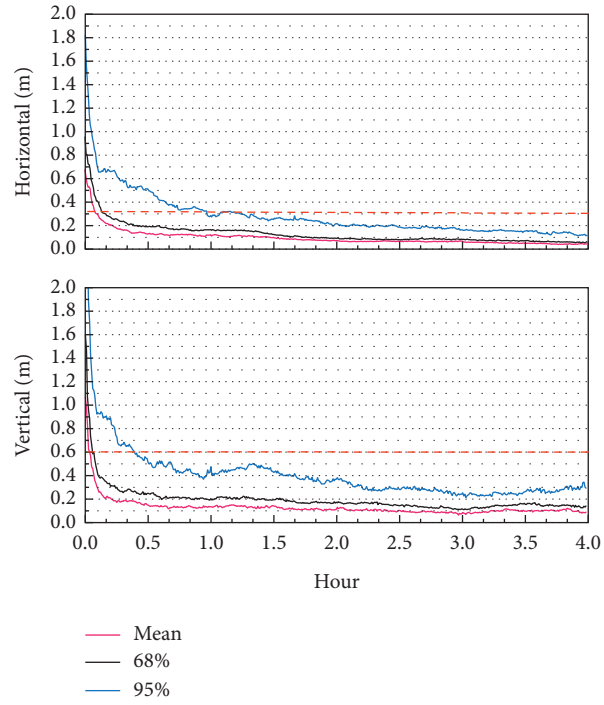

Figure 10: Previous-4-hours convergence statistic of BDS PPP based on BDS PPP-B2b SSR.

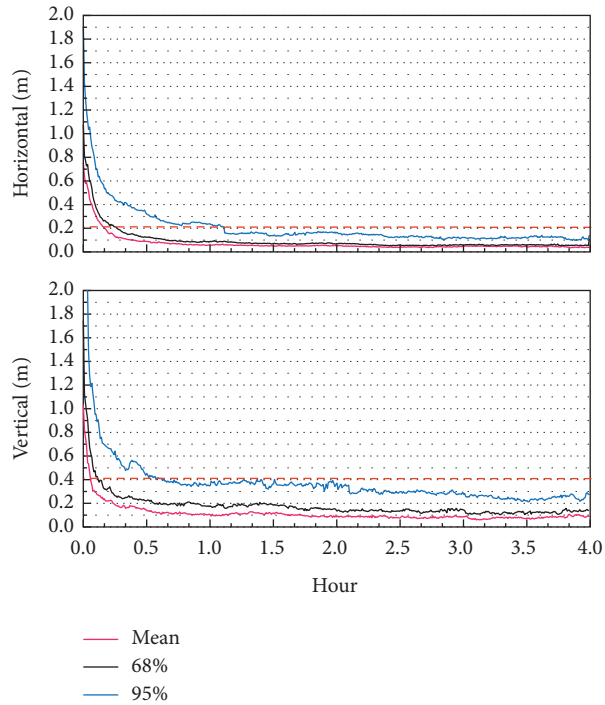

Figure 11: Previous-4-hours convergence statistic of BDS + GPS PPP based on BDS PPP-B2b SSR.

PPP, respectively. Table 5 shows the convergence comparison of BDS PPP and BDS + GPS combined with PPP based on BDS PPP-B2b SSR messages under those two conditions. From Figures 10 and 11 and Table 5, we can find that BDS PPP based PPP-B2b SSR can converge to 30 cm in horizontal direction and 60 cm in vertical direction after an average of 5 minutes and 2.5 minutes, separately. BDS + GPS PPP based on PPP-B2b SSR can converge to 20 cm in horizontal direction and 40 cm in vertical direction after an average of 10 minutes and 3.5 minutes, separately. 68% statistic results show it takes 8.5 minutes in horizontal and 3.5 minutes in vertical direction to achieve the BDS PPP convergence

Table 5: Convergence statistic of BDS PPP and BDS + GPS PPP based on BDS PPP-B2b SSR.

Mode	Condition	Convergence (min)			Improvement rate		
		Mean	68%	95%	Mean	68%	95%
BDS	H (20 cm)	11.5	20.5	118	—		
	V (40 cm)	4.5	6.5	54.5			
	H (30 cm)	5	8.5	58			
	V (60 cm)	2.5	3.5	23.5			
BDS + GPS	H (20 cm)	10	15.5	66.5	13.04%	24.39%	43.64%
	V (40 cm)	3.5	7	37	22.22%	−7.69%	32.11%
	H (30 cm)	6	8	31	−20.00%	5.88%	46.55%
	V (60 cm)	2	4	15.5	20.00%	−14.29%	34.04%
Average	—						39.09%

Table 6: Accuracy statistic of BDS PPP and BDS + GPS PPP based on BDS PPP-B2b SSR.

Mode		Accuracy (cm)			Improvement rate		
		Mean	68%	95%	Mean	68%	95%
BDS	H	7.93	10.83	19.41	—		
	V	12.43	18.51	34.99			
BDS + GPS	H	5.24	7.01	13.08	33.92%	35.27%	32.61%
	V	10.6	16.49	31.19	14.72%	10.91%	10.86%

described in BDS OS PS and 15.5 minutes and 7 minutes for BDS + GPS PPP.

As a comparison, the convergence of BDS PPP and BDS + GPS PPP under same condition is also analysed and those improvements are shown in Table 5. From Table 5, there is a difference of several epochs for the two positioning modes in normal situations. However, for most cases like 95%, GPS corrections of PPP-B2b SSR can promote convergence significantly with average 40% improvement rate for 95% epochs.

Table 6 provides accuracy statistic of BDS PPP and BDS + GPS combined with PPP based on BDS PPP-B2b SSR messages after convergence. From Table 6, we can find that BDS PPP based on PPP-B2b SSR can achieve an average of 7.93 cm in horizontal and 12.43 cm in vertical direction after convergence. The 68% statistic results, the common statistic percentage, show that the accuracy of BDS PPP is 10.83 cm and 18.51 cm in horizontal and vertical direction, while the BDS + GPS PPP is 7.01 cm and 16.49 cm, separately. The 95% statistic results show that the two positioning modes can satisfy the BDS open service performance standard, i.e., 30 cm in horizontal and 60 cm in vertical direction for BDS PPP and 20 cm and 40 cm for BDS + GPS PPP. BDS + GPS PPP based on PPP-B2b SSR can improve positioning accuracy compared to BDS PPP significantly, and the improvement rate is about 34% in horizontal and 12% in vertical direction.

5. Conclusions

The BDS PPP service based on PPP-B2b SSR is introduced in this paper firstly, including the recovery theory of PPP-B2b SSR messages and decoding process. Then the signal-in-space coverage and augmentation accuracy of BDS PPP-B2b SSR are evaluated. Finally the positioning performance of PPP-B2b SSR is analysed based on GNSS tracking stations. The experiment results show the following:

(1) The BDS PPP-B2b signal can provide PPP service for the most area of 65°E–160°E, 15°S–70°N. After combining GPS, the coverage is further expanded to 50°E–180°E, 30°S–70°N.

(2) BDS PPP-B2b SSR can improve signal-in-space accuracy significantly with 40% improvement on BDS orbit, 77% improvement on BDS clock offset, 80% on GPS orbit, and 61% on GPS clock offset. The average SISRE of BDS-3 and GPS is 7.10 cm and 7.58 cm, respectively.

(3) The 95% positioning results show that centimeter- to decimeter-level positioning can be achieved after a few minutes of convergence based on PPP-B2b SSR. Combining GPS corrections can reduce about 40% convergence time compared to single BDS PPP and can further improve positioning accuracy.

As an open service, the BDS PPP-B2b service will further promote mass high-precision applications in mass-market, including autonomous vehicles and precision agriculture.

Data Availability

GNSS products used in this study are available from GFZ (https://ftp.gfz-potsdam.de) and other data used to support the findings of this study are available on request from the corresponding author.

Conflicts of Interest

The authors declare that there are no conflicts of interest regarding the publication of this paper.

Acknowledgments

This research was funded by Beijing Key Laboratory of Urban Spatial Information Engineering (No. 20210223), Young Elite Scientists Sponsorship Program by CAST (2020-2023), Project funded by China Postdoctoral Science Foundation (2021M690192), Beijing Postdoctoral Research Foundation (2021-ZZ-088), and Beijing Nova Program (Z211100002121068).

References

[1] G. Wübbena, M. Schmitz, and A. Bagge, "PPP-RTK: precise point positioning using state-space representation in RTK networks," in *Proceedings of the ION GNSS 2005*, pp. 2584–2594, Institute of Navigation, Long Beach, CA, USA, 2005.

[2] B. Zhang, Y. Chen, and Y. Yuan, "PPP-RTK based on undifferenced and uncombined observations: theoretical and practical aspects," *Journal of Geodesy*, vol. 93, no. 8, pp. 1011–1024, 2019.

[3] J. F. Zumberge, M. B. Heflin, D. C. Jefferson, M. M. Watkins, and F. H. Webb, "Precise point positioning for the efficient and robust analysis of GPS data from large networks," *Journal of Geophysical Research: Solid Earth*, vol. 102, no. B3, pp. 5005–5017, 1997.

[4] L. Chen, Q. Zhao, Z. Hu et al., "GNSS global real-time augmentation positioning: real-time precise satellite clock estimation, prototype system construction and performance analysis," *Advances in Space Research*, vol. 61, no. 1, pp. 367–384, 2018.

[5] X. Li, M. Ge, X. Dai et al., "Accuracy and reliability of multi-GNSS real-time precise positioning: GPS, GLONASS, BeiDou, and Galileo," *Journal of Geodesy*, vol. 89, no. 6, pp. 607–635, 2015.

[6] Galileo Gnss Agency, *GNSS User Technology Report. Issue 3*, Publications Office of the EU, Galileo GNSS Agency, Paris, France, 2020.

[7] Galileo Gnss Agency, *Galileo High Accuracy Service (HAS)*, Publications Office of the EU., Galileo GNSS Agency, Paris, France, 2020.

[8] Cabinet Office, *Quasi-Zenith Satellite System Interface Specification Centimeter Level Augmentation Service (IS-QZSS QZSS-L6-003)*, Cabinet office, Japan, 2020.

[9] Cabinet Office, *Quasi-Zenith Satellite System Performance Standard (PS-QZSS-002)*, Cabinet office, Japan, 2020.

[10] J. Barrios, J. Caro, J. Calle et al., "Update on Australia and New Zealand DFMC SBAS and PPP system results," in *Proceedings of the 33th International Meeting of the Satellite Division of The Institute of Navigation (ION GNSS+ 2018)*, Miami, Florida, September 2018.

[11] H. Rui and F. Ignacio, "Open format specifications for PPP/PPP-RTK services: overview and interoperability assessment," in *Proceedings of the ION GNSS 2020 of Institute of Navigation*, pp. 1268–1290, September 2020.

[12] China Satellite Navigation Office, *Development of the BeiDou Navigation Satellite System*, China Satellite Navigation Office, China, 2019.

[13] China Satellite Navigation Office, *BeiDou Navigation Satellite System Open Service Performance Standard*, China Satellite Navigation Office, China, 2021.

[14] China Satellite Navigation Office, *BeiDou Navigation Satellite System Signal in Space Interface Control Document Precise Point Positioning Service Signal PPP-B2b*, China Satellite Navigation Office, China, 2020.

[15] K. Asari, S. Matsuoka, and H. Amitani, "QZSS RTK-PPP application to autonomous cars," in *Proceedings of the ION GNSS+ 2016*, pp. 2136–2142, Institute of Navigation, Portland, Oregon, 2016.

[16] Iso 18197:2015(E), *Space Systems–Space Based Services Requirements for Centimeter Class Positioning*, International Organization for Standardization, London, UK, May 2015.

[17] Z. Nie, X. Xu, Z. Wang, and J. Du, "Initial assessment of BDS PPP-B2b service: precision of orbit and clock corrections, and PPP performance," *Remote Sensing*, vol. 13, no. 11, Article ID 2050, 2021.

[18] P. Teunissen and O. Montenbruck, *Handbook of GNSS*, Springer Nature, Switzerland, 2017.

[19] P. S. Gps Sps, *Global Positioning System Standard Positioning Service Performance Standard*, Department of Defense United States of America, VA, USA, April 2020.

[20] O. Montenbruck, P. Steigenberger, and A. Hauschild, "Broadcast versus precise ephemerides: a multi-GNSS perspective," *GPS Solutions*, vol. 19, no. 2, pp. 321–333, 2015.

[21] P. Steigenberger and O. Montenbruck, "Consistency of MGEX orbit and clock products," *Engineering*, vol. 6, no. 8, pp. 898–903, 2020.

[22] P. Rebischung and R. Schmid, *IGS14/igs14.atx: A New Framework for the IGS Products*, American Geophysical Union Fall Meeting 2016, San Francisco, USA, 2016.

[23] M. Ge, J. Chen, J. Douša, G. Gendt, and J. Wickert, "A computationally efficient approach for estimating high-rate satellite clock corrections in realtime," *GPS Solutions*, vol. 16, no. 1, pp. 9–17, 2012.

[24] L. Chen, M. Li, Y. Zhao, Z. Hu, F. Zheng, and C. Shi, "Multi-GNSS real-time precise clock estimation considering correction of inter-satellite code bias," *GPS Solutions*, vol. 25, no. 2, 2021.

[25] O. Montenbruck, P. Steigenberger, L. Prange et al., "The multi-GNSS experiment (MGEX) of the international GNSS service (IGS) - a," *Advances in Space Research*, vol. 59, no. 7, pp. 1671–1697, 2017.

[26] R. Dach, S. Schaer, and U. Hugentobler, "Combined multi-system GNSS analysis for time and frequency transfer," in *Proceedings of the 20th European Frequency and Time Forum EFTF06*, pp. 530–537, Braunschweig, Germany, March 2006.

[27] N. Wang, Y. Yuan, Z. Li, O. Montenbruck, and B. Tan, "Determination of differential code biases with multi-GNSS observations," *Journal of Geodesy*, vol. 90, no. 3, pp. 209–228, 2016.

[28] L. Chen, M. Li, and Z. Hu, "Method for real-time self-calibrating GLONASS code inter-frequency bias and improvements on single point positioning," *GPS Solutions*, vol. 22, no. 4, Article ID 111, 2018.

[29] L. Chen, W. Jiao, X. Huang et al., "Study on signal-in-space errors calculation method and statistical characterization of BeiDou navigation satellite system," *Lecture notes in electrical engineering*, vol. 243, pp. 423–434, 2013.

[30] X. Li, Y. Yuan, Y. Zhu et al., "Precise orbit determination for BDS3 experimental satellites using iGMAS and MGEX tracking networks," *Journal of Geodesy*, vol. 93, no. 7, pp. 103–117, 2019.

[31] M. Ge, G. Gendt, M. Rothacher, C. Shi, and J. Liu, "Resolution of GPS carrier-phase ambiguities in precise point positioning (PPP) with daily observations," *Journal of Geodesy*, vol. 82, no. 7, pp. 389–399, 2008.

[32] J. Wu, S. Wu, G. Hajj, W. Bertiger, and S. Lichten, "Effects of antenna orientation on GPS carrier phase," *Manuscripta Geodaetica*, vol. 18, no. 2, pp. 91–98, 1993.